

Determination of polyglycerol substructures and their connectivity by multidimensional and quantitative NMR spectroscopy

Downloaded from: https://research.chalmers.se, 2026-11-08 07:57 UTC

Citation for the original published paper (version of record):
Bilén, F., Nahavandizadeh, N., Larsson, M. et al (2026). Determination of polyglycerol substructures and their connectivity by multidimensional and
quantitative NMR spectroscopy. Polymer Chemistry, 17(39): 4311-4322.
http://dx.doi.org/10.1039/d6py00638h

N.B. When citing this work, cite the original published paper.

research.chalmers.se offers the possibility of retrieving research publications produced at Chalmers University of Technology. It covers all kind of research output: articles, dissertations, conference papers, reports etc. since 2004. research.chalmers.se is administrated and maintained by Chalmers Library

(article starts on next page)

Polymer Chemistry

ROYAL SOCIETY OF CHEMISTRY

PAPER

Published on 18 September 2026
Licensed under CC-BY 4.0

Check for updates

Cite this: *Polym. Chem.*, 2026, **17**, 4311

Determination of polyglycerol substructures and their connectivity by multidimensional and quantitative NMR spectroscopy

Frida Bilén, †[a] Nasim Nahavandizadeh, †[a,b] Moa Larsson, [a] Sami Zeliouche, *[a,b,c] Romain Bordes *[a] and Lars Evenäs *[a,b,c]

Received 2nd July 2026,
Accepted 6th September 2026

DOI: 10.1039/d6py00638h

rsc.li/polymers

Polyglycerol (PG) is a versatile polyether whose properties strongly depend on its molecular weight and constitutional architecture. However, detailed characterization of its molecular constitution remains challenging due to its inherent heterogeneity and the resulting spectral overlap in NMR experiments. In this work, we present an approach for the assignment and quantitative analysis of PG substructures using NMR spectroscopy. A detailed assignment of ^{13}C NMR signals was achieved, enabling identification of glycerol units based on both connectivity (terminal, linear, dendritic) and linkage type (*via* primary or secondary carbons). The assignments further reveal the identities of connected glycerol units, enabling characterization of local constitutional environments in addition to individual glycerol substructures. This provides a more comprehensive description than conventional methods. Based on these assignments, a user-friendly protocol was established to quantify the relative abundance of PG substructures. Applying this methodology to four oligomeric PG samples (PG2–PG6) reveals an increasing proportion of linear units with molecular size and a predominance of primary linkages, consistent with mostly linear molecules. The results also reveal an increasing diversity of constitutional substructures with increasing molecular size. A simplified ^{1}H NMR approach is further introduced for rapid estimation of terminal and linear content. This work provides a broadly applicable framework for quantitative constitutional characterization of polyglycerol, enabling improved understanding of its structure and supporting future studies of structure–property relationships.

1 Introduction

Polyglycerol (PG) is an oligomeric or polymeric substance composed of glycerol units linked through various ether bond arrangements, resulting in a wide range of molecular architectures and sizes. Its structures span from small oligomers, such as diglycerols containing only two glycerol units, to large and sometimes hyperbranched polymers comprising more than ten thousand repeating units.[1,2]

Polyglycerol is used in a wide range of applications, partly due to its high biocompatibility[3] and many hydroxyl groups that makes it highly water soluble and provide potential derivatization sites.[4,5] The different sizes and structures provide many possible uses. The large hyperbranched and dendritic polyglycerols are used in *e.g.* various biomedical applications,[6,7] including as biodegradable nanocarriers in the form of polylactic acid-hyperbranched polyglycerol copolymers.[8] Polyglycerol has been explored as a multifunctional alternative to poly(ethylene glycol) (PEG), with the advantage of offering additional sites for further chemical modification.[5,9,10] Beyond these, polyglycerol-based materials of various structures have found use in additive manufacturing[11] and in water-based printing inks.[12] At the oligomeric scale, polyglycerol and its derivatives have a broad range of established and emerging applications. Fatty acid esters of polyglycerol are used as green, nonionic surfactants,[13,14] and polyglycerol esters are widely used as food emulsifiers.[15] Triglycerol is used as a moisturizing agent in cosmetics,[6] and polyesters derived from di- and triglycerol have additionally shown promise as lubricants.[16] More broadly, oligomeric polyglycerol represents a growing market, with key applications spanning the personal care, food and beverage, and pharmaceutical industries.[17]

While, as the name suggests, PG can be prepared by condensation of glycerol, it can also be synthesized from other monomers, see Fig. 1a, each of which promotes the formation of different PG structures. For the preparation of large, hyperbranched PG, glycidol is commonly employed as a monomer.[18] The epoxide group offers a reactive functional

[a]*Department of Chemistry and Chemical Engineering, Chalmers University of Technology, Gothenburg, Sweden. E-mail: sami.zeliouche@chalmers.se, bordes@chalmers.se, lars.evenas@chalmers.se*
[b]*Wallenberg Wood Science Center, Chalmers University of Technology, Gothenburg, Sweden*
[c]*FibRe Centre for Lignocellulose-based Thermoplastics, Chalmers University of Technology, Gothenburg, Sweden*
† These authors contributed equally to this work.

group that can take part in the polymerization. The use of glycidol allows PG to reach very high molecular weight, but a significant drawback is the toxic nature of glycidol.[19,20] Other synthetic strategies to achieve hyperbranched polyglycerol are using glycerol carbonates.[21] In contrast, linear PG can be synthesized by polymerizing hydroxyl-protected glycidol derivatives, such as ethoxyethyl glycidyl ether (EEGE), followed by removal of the protecting group after polymerization.[5,22] There are also examples where glycidol and the protected monomer have been used together in various relative amounts to control the degree of branching.[23]

Polyglycerol can also be produced from glycerol, a renewable raw material that is generated in large quantities as the main byproduct of biodiesel production. Valorization of this glycerol side stream contributes not only to the sustainability of polyglycerol production but also to the improved economic viability of the biodiesel industry.[24] Although linear products are favored during the conventional base catalyzed self-polymerization of glycerol due to the more reactive primary hydroxyl groups and the regioselective ring opening of formed epoxide,[25] it yields a mixture of isomers resulting from the three hydroxyl groups that can participate in etherification.[15] Consequently, PG is typically obtained as a mixture of molecules with different molecular weights and varying degrees of linear, branched, and cyclic structures, see Fig. 1b for two examples. The resulting size distribution and degree of branching can be influenced by the choice of catalyst and reaction conditions.[10,19,26,27] Etherification of glycerol typically yields oligomers of relatively low molecular weight due to formation of undesired side products and slow reaction rate compared to polymerization of glycidol.[28] Nevertheless, Salehpour and Dubé reported the polymerization of glycerol to PG with a number-average molecular weight corresponding to approximately 50 glycerol units, demonstrating that moderately high degree of polymerization can also be achieved directly from glycerol.[19]

The molecular structure and degree of branching of PG has a direct effect on its physicochemical properties. Imran ul-haq *et al.* showed that for high molecular weight PG (120 000 g mol^{-1}, *ca.* 1600 glycerol units) considered for drug delivery systems, hyperbranched PG has longer blood circulation time than its linear counterpart, attributed partly to the higher deformability of the linear molecule which allows it to be more easily filtered out by the kidneys.[29] For partially esterified linear or branched PG (3000 g mol^{-1}, *ca.* 40 glycerol units) used for encapsulation, it has been shown that the PG structure has an effect on the viscosity and encapsulation capacity.[30] The degree of branching also affects glass transition temperature, and increased branching seems to increase the intramolecular hydrogen bonding while decreasing the intermolecular hydrogen bonding.[23] In addition, structural variations in branched PG influence interfacial and functional properties such as wettability and print quality when used as a print additive,[12] and plasma protein adsorption when used in biocompatible surfaces.[31] The heterogeneous nature of polyglycerol materials poses challenges for establishing structure–property relationships. Zhang and Zhang have for example raised concerns about the lack of understanding of the effect of polyglycerol branching on surfactant properties for polyglycerol ester surfactants.[13] These challenges underscore the importance of quantitative structural characterization of polyglycerol.

NMR spectroscopy has been used to determine information about polyglycerol structure. The first characterization of various polyglycerol structures from ^{13}C NMR was done in the 1980s.[32,33] These assignments enabled only partial structural characterization, however. Subsequent studies have progressively extended the peak assignment for structural identification,[21,34–37] with the most intense peaks assigned to one or several of the six glycerol unit structures shown on the top row of Table 1. These structures have been categorized according to the number of ether linkages to other glycerol units, where a structure with all three carbons linked is called dendritic (D), with two links is called linear (L), with one link is called terminal (T), and no links is a glycerol molecule (G). The structures can be divided further according to by which carbon(s) they are connected, and this nomenclature varies between different references, but we have chosen to name them according to whether they are connected *via* their

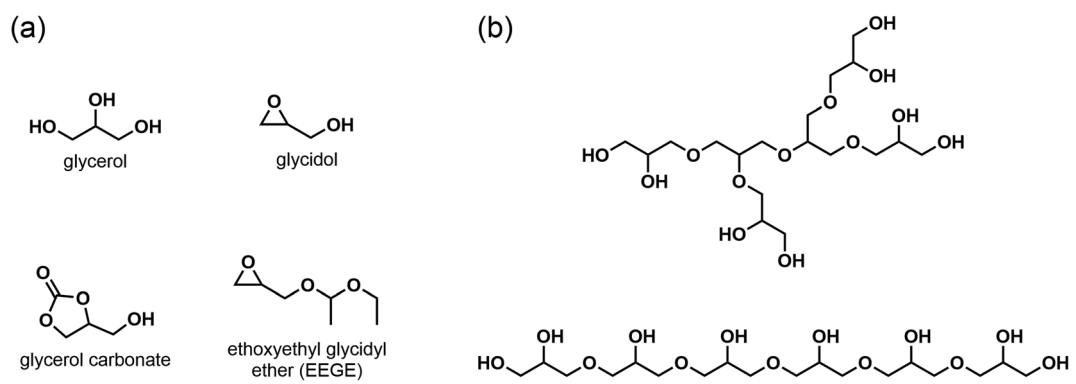
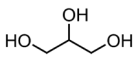
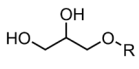
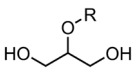
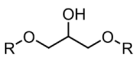
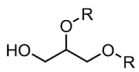
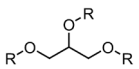
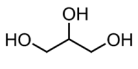
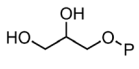
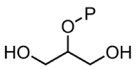
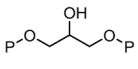
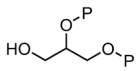
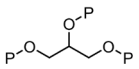
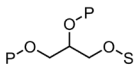
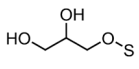
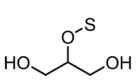
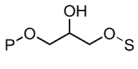
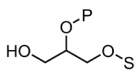
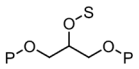
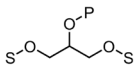
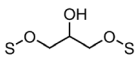
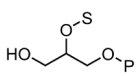
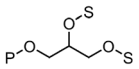
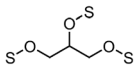
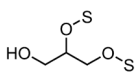


Fig. 1 (a) Four examples of monomers used to synthesize polyglycerol, and (b) two examples of polyglycerol molecules, each with six glycerol units but one is linear and one branched.

 This journal is © The Royal Society of Chemistry 2026

Table 1 Overview of possible glycerol units and substructures in polyglycerol (PG)

	G	Tp	Ts	Lpp	Lsp	D	
Structure							
Glycerol units needed to form the structure	1	2	2	3	3	4	
Substructure	 G	 Tp-p	 Ts-p	 Lpp-pp	 Lsp-pp	 Dpsp-ppp	 Dpsp-pps
		 Tp-s	 Ts-s	 Lpp-ps	 Lsp-ps	 Dpsp-psp	 Dpsp-sps
				 Lpp-ss	 Lsp-sp	 Dpsp-pss	 Dpsp-sss
					 Lsp-ss		

G = glycerol (not connected to any other glycerol unit, three free hydroxyl groups), T = terminal (one connection to another glycerol unit, two free hydroxyl groups), L = linear (two connections, one free hydroxyl group), and D = dendritic (three connections, no free hydroxyl groups). In the unit notation (*e.g.*, Tp-p, Ts-p, Lpp-pp), the letter(s) before the hyphen indicates whether the linkage occurs *via* a primary (p) or secondary (s) carbon of the unit, while the letter(s) after the hyphen denote the corresponding carbon(s) of the connected glycerol unit. For structures with multiple linkages, the correspondence is pairwise: the first letter before the hyphen corresponds to the first letter after the hyphen, the second letter before the hyphen corresponds to the second letter after the hyphen, and so forth.

primary (p) or secondary (s) carbons. Building on these assignments, Sunder *et al.* developed a widely adopted method for calculating the degree of branching from quantitative ^{13}C NMR integrals of dendritic and linear glycerol unit structures.[36] For PG synthesized with a distinct initiator molecule, the degree of polymerization has also been determined by comparing the integrals of the initiator peaks to the rest of the polyglycerol, in either ^{13}C[36] or ^{1}H NMR.[23]

Although these peak assignments of PG provide useful information, it does not give a complete connectivity description of the often heterogeneous PG material. As has been shown by Cassel *et al.*[38] by comparing the NMR signals for several pure oligomeric PG standards, carbons belonging to different glycerol unit structures sometimes give signals at similar chemical shifts, giving rise to a complex pattern of partially overlapping signals. In addition, they showed that the chemical shifts for a given glycerol unit structure are sensitive to the constitution of the neighboring units, and in theory it could then be possible to extract more detailed structural information from the NMR spectra than what has been done so far. The reported ^{13}C NMR chemical shift of the standards by Cassel *et al.* gives important information in the attempt to characterize the structure of a PG material on a deeper structural level, but they cover only a limited set of oligomers, which does not represent the full structural space of larger or more branched polyglycerols. Therefore, we present a developed methodology for quantitative determination of detailed constitutional information of PG.

In this work, we conduct a multi-experiment NMR strategy for peak assignment in ^{13}C NMR, which is then used for quantification of glycerol substructures in PG. This provides detailed constitutional information at the level of individual glycerol units and their connectivity. By combining ^{13}C, DEPT-135, INADEQUATE, HSQC, and HMBC NMR experiments, we identify substructures that describe not only the local glycerol unit configuration, but also the identity of the connecting carbon on the adjacent glycerol unit (see Table 1). These substructures are classified according to whether the connecting carbon on the neighboring unit is primary (p) or secondary (s), thereby offering a more comprehensive picture of PG constitution. The resulting assignments are compared to previously published PG peak assignments, demonstrating that they provide a complementary and more informative basis for PG structure elucidation. Building on these assignments, we propose a quantification protocol based on quantitative ^{13}C 1D NMR spectrum and apply it to four oligomeric PG samples of varying composition.

Finally, for cases where this level of structural detail is unnecessary, we present a straightforward ^{1}H 1D NMR spectrum approach for rapid assessment of terminal and linear glycerol units.

2 Results and discussion

Four different oligomeric polyglycerol samples were investigated, PG2, PG3, PG4 and PG6, with increasing size and polydispersity. See Fig. 2 for the ^{13}C spectra of the four samples and for pure glycerol. ^{1}H, ^{13}C and DEPT-135 spectra for the four samples and glycerol can be found in the SI.

2.1 Assignment of ^{13}C NMR signals

Both PG2, representing the smallest oligomers with the most narrow size distribution, and PG6, representing the largest oligomers with the widest size distribution, were used for the peak assignment, in combination with pure glycerol. Together, these three samples provided a comprehensive basis for the assignment, as each contained signals not present or well-resolved in the other spectra.

Three main regions could be identified in the ^{13}C spectra based on the chemical shift: a high-shift region corresponding to secondary CH-OR carbons, a middle-shift region containing both secondary CH-OH and primary CH_2-OR carbons, and a low-shift region corresponding to primary CH_2-OH carbons.[38] For the middle region, where CH and CH_2 carbons overlap, the DEPT-135 pulse sequence was used to distinguish between the two carbon types.

One-bond carbon–carbon ($^{1}J_{CC}$) connectivity was then established through the INADEQUATE pulse sequence. However, due to the low natural abundance of ^{13}C and the consequently low sensitivity of this experiment, only a subset of the signals could be assigned this way. For the remaining low intensity signals, HSQC and HMBC were employed to complete the assignment by establishing short- and long-range carbon-proton ($^{n}J_{CH}$) connectivities. The HSQC and HMBC spectra of PG6, and one representative example illustrating this assignment process is provided in the SI.

Using this combined approach, most signals could be assigned to the carbon atoms of the glycerol unit substructures presented in Table 1. For some peaks of low intensity or overlapping signals, a resolved assignment was not attainable, and instead several substructures were attributed to the same multi-signal containing peak, and some signals remained unassigned. The resulting chemical shift assignment is presented in Fig. 3.

An intriguing observation is that even within the same substructure, the chemical shifts can vary quite noticeably. This was particularly noticeable for the terminal substructures, where two slightly different sets of peaks were consistently observed, marked with prime (′) or double prime (″) in Fig. 3. This may reflect differences in the chemical environment beyond the directly connected glycerol units. Such differences could arise from longer-range constitutional effects, but stereochemical sequence may also contribute, since condensation can generate stereogenic environments and hence diastereomeric oligomer sequences. The present NMR data establish constitutional connectivity but do not allow these two contributions to be distinguished unambiguously.

No peaks were assigned to dendritic, Lsp, or Lpp-ss substructures for the four samples, though a small number of unassigned peaks remain that may correspond to these units.

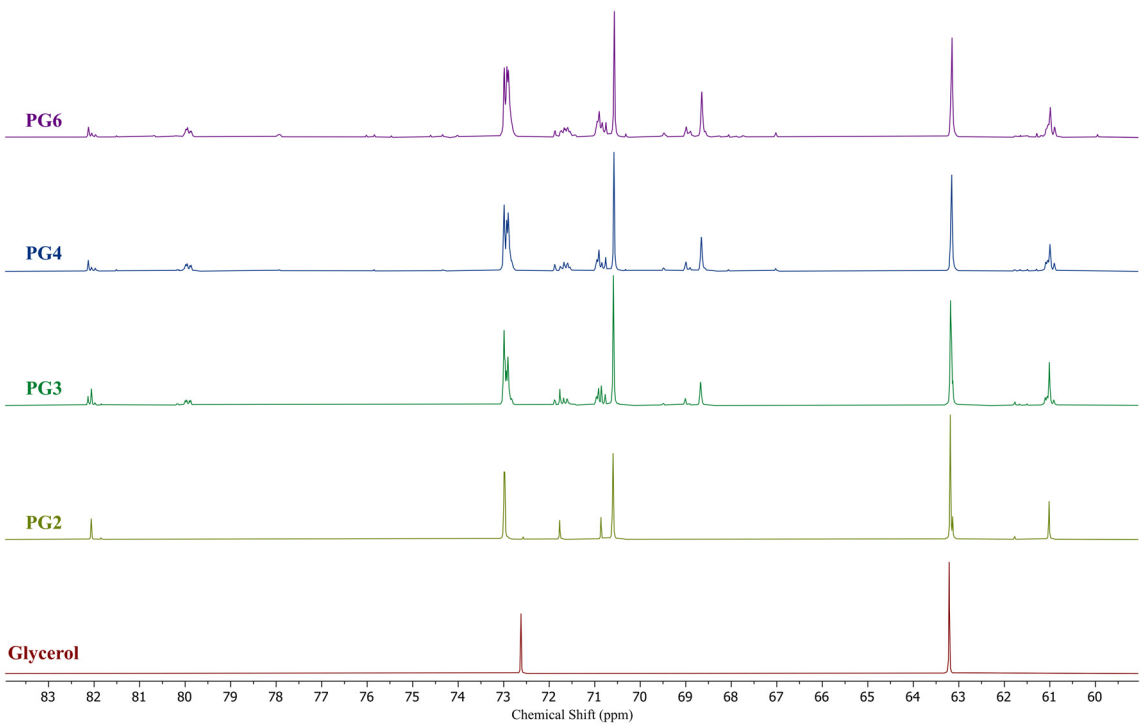


Fig. 2 Quantitative 201 MHz ^{13}C NMR spectra of glycerol and the four polyglycerol samples (PG2, PG3, PG4, and PG6) recorded in DMSO-d_6.

This journal is © The Royal Society of Chemistry 2026

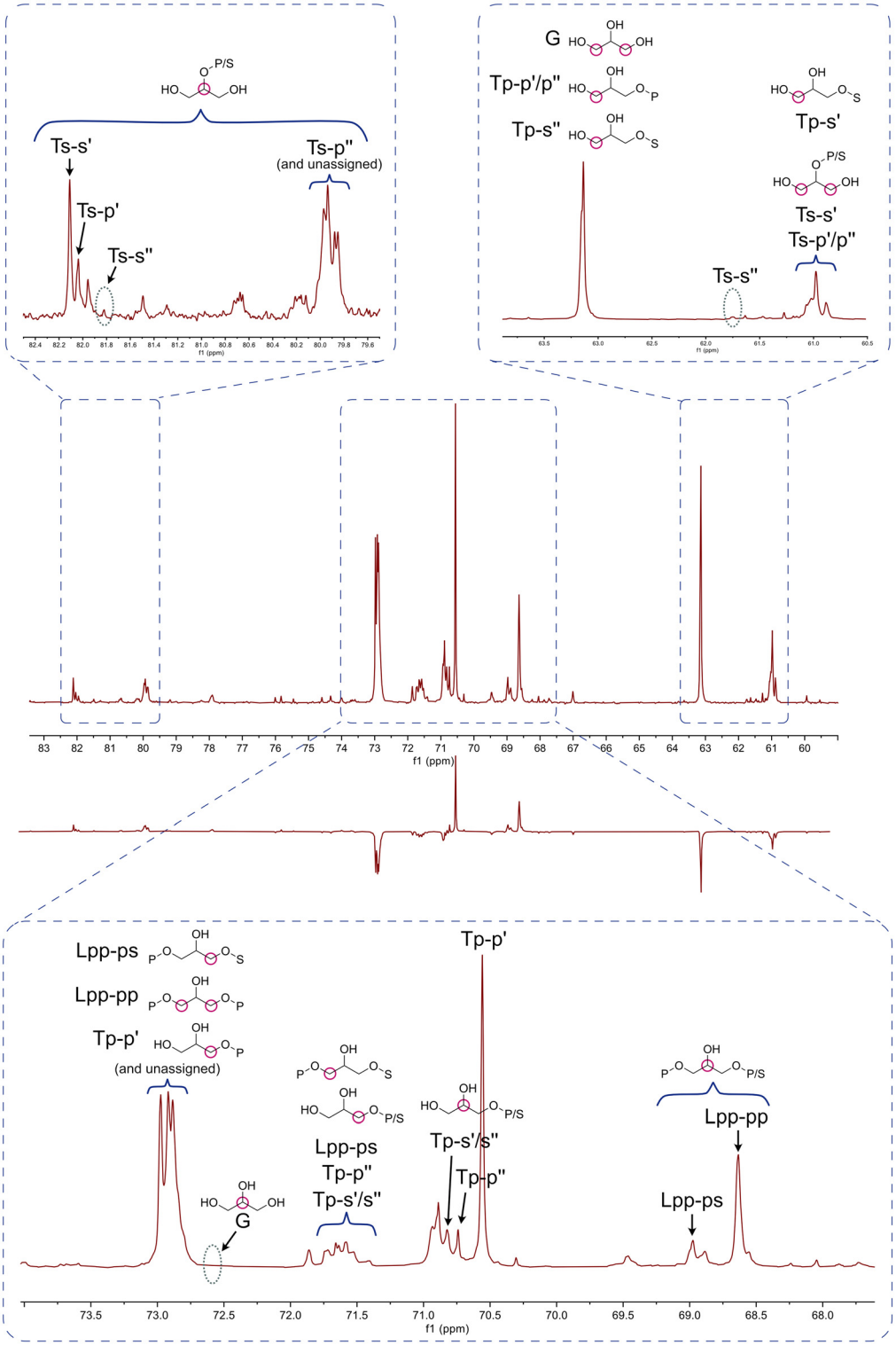


Fig. 3 Visualization of the assigned peaks, shown on the 201 MHz ^{13}C NMR spectrum of PG6. Dotted circles indicate assignments based on the PG2 sample that are either absent or below the signal-to-noise threshold in the PG6 spectrum. The DEPT-135 spectrum, shown below the ^{13}C spectrum, was used to distinguish between CH_2 carbons (negative peaks) and CH carbons (positive peaks). Structures marked with prime (') or double prime ('') within the same substructure type indicate two slightly different sets of chemical shifts, which may arise from differences in the longer-range constitutional and/or stereochemical environment.

The lack of dendritic structures is consistent with the nature of the materials studied, as the samples have a low degree of polymerization and were intentionally produced to be predominantly linear. For future work aiming to complete the spectral assignment for these substructures, the strategy developed here could be applied to more highly branched polyglycerol materials, or alternatively the assignments could possibly be deducted by comparison with previously reported NMR data for branched structures in the literature.

The comparison between the peak assignments presented here with selected literature references is shown in Fig. 4. The comparison with the work by Cassel *et al.*,[38] who report assignments at the same detailed substructural level for pure PG oligomer standards, is particularly important. The two studies differ methodologically in an important respect: Cassel *et al.* assign peaks for known, pure structures, whereas our materials are mixtures of unknown constitution. In addition, the chemical shifts cannot be compared directly, as they are concentration-dependent and differ between the two datasets. In general, we observe that peaks shift downfield with increasing concentration (see Fig. S12 in SI), though the magnitude of this effect varies between individual carbon signals, reflecting differences in how sensitive each chemical environment of the nuclei is to concentration. Since Cassel *et al.* do not report the concentration used in their measurements, an exact shift-by-shift comparison is not possible. In this work, the concentrations used are reported explicitly, which should facilitate direct comparisons in future studies. When the shifts are adjusted to match the position of common peaks as reference points, however, most major peaks align well between the two works, which we regard as a validation of our assignment strategy.

The two studies are complementary to each other, and together the two datasets cover a broad subset of possible PG constitutions. Notably, some assignments from Cassel *et al.* offer potential explanations for peaks that remain unassigned in our spectra. For example, the cluster of small peaks between 61 and 62 ppm may correspond to Lsp or Ts structures, and the unassigned component of the peak just below 73 ppm is consistent with dendritic or Lsp units. While the reference assignments of Cassel *et al.* support the interpretation of ambiguous or low-intensity signals in our spectra, our methodology demonstrates how assignments can be systematically done for mixtures of various PG molecules. This complementarity is significant for the broader PG community, where Cassel *et al.* provide validated reference assignments for key substructures, and our work expands the accessible structural space of PG and equips the community with both validated reference points and a practical, transferable analytical protocol for future assignment efforts. Together, this enables more reliable and detailed structural characterization of PG materials, which is essential for advancing structure–property relationships and supporting the rational design of PG-based materials.

The assignments reported by Sunder *et al.*[36] have been widely adopted for determining PG structure, and are shown in Fig. 4 alongside the more recent complementary work of Spears *et al.*,[37] which follows the same assignment but with an additional Ts structure. A key difference to our work is that Sunder *et al.* worked with larger, hyperbranched PG, which produces a different spectral response with more linear and dendritic structures compared to the low-molecular-weight, predominantly linear materials studied here. Our results and those of Cassel *et al.* suggest that the approach used by Sunder *et al.* of grouping broad regions of overlapping signals under one or two structural assignments is a simplification of the underlying spectral complexity. As shown in both datasets,

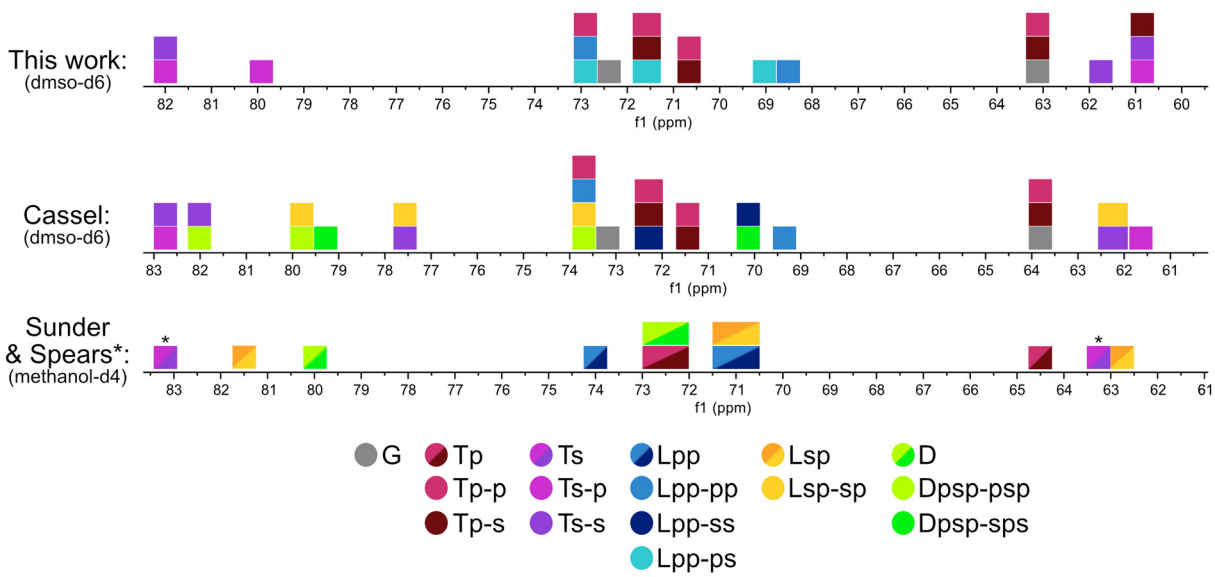


Fig. 4 Comparison of the ^{13}C peak assignments from this work (based on glycerol, PG2, and PG6) with those reported by Cassel *et al.*[38] and Sunder *et al.*[36] supplemented with additional assignments from Spears *et al.*[37] Since the spectra were recorded in different solvents and at different concentrations, which directly affects the chemical shifts, the axes have been adjusted to facilitate visual comparison of the assignment positions across studies.

This journal is © The Royal Society of Chemistry 2026

several of these regions contain contributions from multiple distinct substructures. The Sunder assignment scheme remains useful for a rough compositional analysis, but where more detailed structural information is required, the assignments developed here and by Cassel *et al.* offer a valuable complement.

2.2 Quantitative constitutional analysis based on ^{13}C NMR

Inverse-gated quantitative ^{13}C spectra were collected by assuring that the relaxation delay between scans was sufficient, and the quantitative nature of the spectra enables integrals to be used for determination of the relative amounts of the substructures.

The determination of the relative amounts of each substructure began with the well-resolved peaks that could be uniquely assigned to a single substructure, marked with an asterisk (*) in Table 2. As each carbon in a specific substructure contributes equally to the total integral, the integral contribution for the remaining carbons of this substructure could then be determined and subtracted from peaks with signal overlap, following the procedure in Table 2, where the peak names are specified according to Fig. 5. For substructures Tp-s and Ts-p, however, this approach was insufficient due to multiple peaks with overlap. In these cases, it was assumed that the residual integral of peak M (after subtraction of contributions from G and Tp-p) corresponds to Tp-s, and the residual integral of peak O (after subtraction of contributions from Tp-s and Ts-s) corresponds to Ts-p.

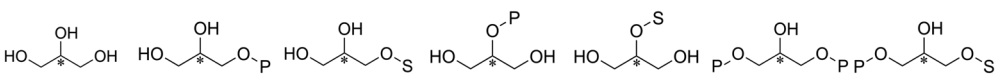
The integrals of each assigned peak and the calculations for the contribution of each substructure can be seen in Table 2 for the PG6 sample. This process was repeated for the other samples as well. The composition of the samples in terms of the different substructures could be determined, see Table 3.

The relative amount of substructures with two ether bridges increases with increasing size of the polyglycerol samples, which is expected since longer chains require a higher proportion of linear or dendritic units to extend the backbone. Correspondingly, the integral contribution from unassigned peaks also increases for larger and wider size distributions, as larger polyglycerol structures give rise to a greater variety of possible connectivity patterns, resulting in a larger number of small peaks with slightly different chemical shifts that are difficult to assign individually. Overall, the findings are in good agreement with the supplier's claim of a high linear content, with Tp-p and Lpp-pp being the most prevalent substructures identified, indicating that the polyglycerol chains are predominantly linearly connected through ether bonds at the primary carbons. The quantitative ^{13}C analysis benefits from high magnetic field strength, as reduced spectral resolution at lower fields increases overlap between closely spaced signals and consequently the uncertainty of deconvoluted integrals. Lower sensitivity can in principle be compensated by longer acquisition times. High-field NMR is therefore recommended when accurate quantification of individual substructures is required.

2.3 Determination of the sample composition based on ^{1}H NMR

Since quantitative ^{1}H NMR is more accessible than quantitative ^{13}C NMR, the former was also investigated as a practical alternative for obtaining compositional information about the

Table 2 Illustration of the stepwise procedure used to determine the fractional composition of G, T, and L substructures in sample PG6, based on peak deconvolution in the ^{13}C NMR spectrum, where the peaks are named according to Fig. 5



	Substructure							
Peak (integral)	Glycerol	Tp-p	Tp-s	Ts-p	Ts-s	Lpp-pp	Lpp-ps	Residual
A (0.010)					= A*			0
B (0.004)				= B*				0
C (0)					= C*			0
D (0.036)				= Y/2-B				0.023
E (0.0310)		= J				= 2L	= K	0.005
F (0)	= F*							0
G (0.057)		= I	= H				= K	0.001
H (0.026)			= H*					0
I (0.015)		= I*						0
J (0.103)		= J*						0
K (0.016)							= K*	0
L (0.072)						= L*		0
M (0.123)	= 2F	= I + J	=M-2F-(I+J) X					0
N (0)					= 2C			0
O (0.074)			= H–X	=O-(H-X)-2A Y	= 2A			0
Unassigned peaks	—	—	—	—	—	—	—	0.191
Glycerol unit fraction	**0**	**0.35**	**0.08**	**0.05**	**0.03**	**0.22**	**0.05**	**0.22**

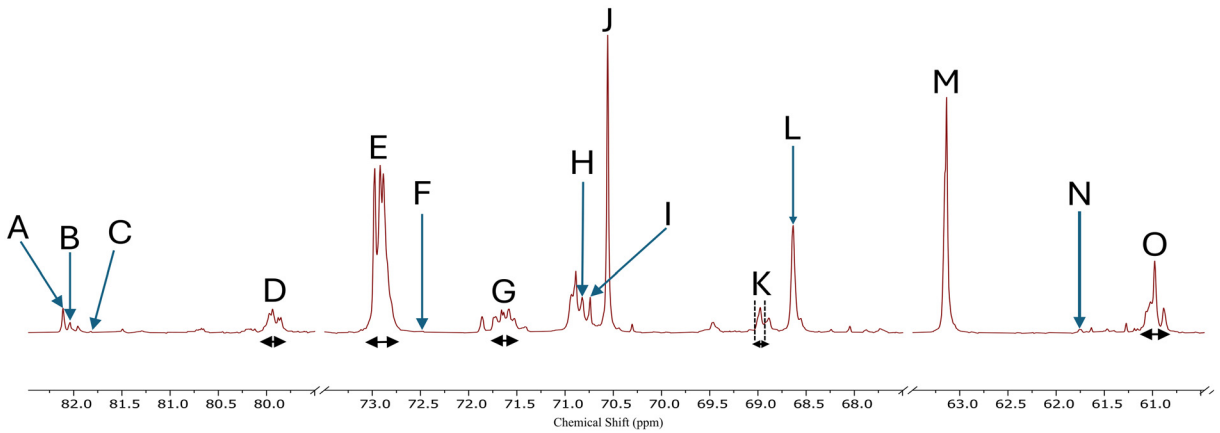
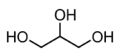
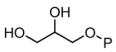
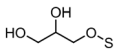
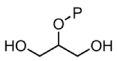
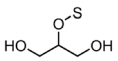
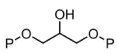
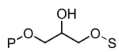


Fig. 5 Naming convention of the assigned signals, visualized on the ^{13}C NMR spectrum of PG6 (201 MHz). Peaks with several overlapping signals that were assigned as a group are marked with double-headed arrows to show the range of signals that are included in the named peak.

Table 3 Quantity of each substructure by ^{13}C NMR spectroscopy

	Quantity of each substructure based on integrals of C signals in ^{13}C spectrum							
Sample	G 	Tp-p 	Tp-s 	Ts-p 	Ts-s 	Lpp-pp 	Lpp-ps 	Unassigned
Glycerol	100%	—	—	—	—	—	—	—
PG2	2%	72%	12%	11%	1%	1%	—	1%
PG3	—	55%	6%	10%	3%	14%	4%	8%
PG4	—	43%	4%	8%	3%	21%	5%	15%
PG6	—	35%	8%	5%	3%	22%	5%	22%

polyglycerol samples. See Fig. 6 for the ^{1}H NMR spectra of the four samples and glycerol.

Quantitative ^{1}H NMR revealed two distinct regions: one between 3.1 and 4.1 ppm corresponding to carbon-bound protons, and one between 4.3 and 5.0 ppm corresponding to hydroxyl protons. The carbon-bound proton region (3.1–4.1 ppm) proved difficult to use for quantification. The signals from different constitution types overlap heavily in this region, and a water peak was also present, further complicating the interpretation of the integration. For these reasons, the hydroxyl region (4.3–5.0 ppm) was used for quantification instead, as it offered better-resolved and more distinguishable signals. DMSO-d_6 was selected as the solvent to enable observation of the hydroxyl protons, as protic solvents such as deuterated alcohol or water would cause rapid exchange with the OH protons, rendering these signals invisible in the ^{1}H NMR spectrum.

Based on the peak assignment from HSQC, three regions could be identified within the hydroxyl range: L at 4.71–4.77 ppm, T + G at 4.43–4.64 ppm, and G at 4.36–4.40 ppm, see Fig. 7. While the terminal and glycerol hydroxyl signals overlap within the T + G region, the G-contribution could be subtracted based on the separate G region to give the terminal hydroxyls (integral of 4.36–4.40 ppm region divided by two, as this region is for both of the primary hydroxyls of the glycerol). Therefore, this region could be used for quantitative analysis to calculate the relative amounts of hydroxyl protons associated with the structures L, T and G. To calculate the relative amounts of each structure, the integrals of these regions should be compared to the integral of the C–H region. However, any present water signal in the C–H region must first be considered. In the glycerol, PG2 and PG3 samples, the water signal was sufficiently resolved to allow estimation of the water contribution. The number of water molecules per glycerol unit (n_{H_2O}) was calculated using the water signal integral (I_{H_2O}) and the integral of the 3.1–4.1 ppm region ($I_{3.1–4.1}$), including five non-exchangeable protons per glycerol unit and two protons per water molecule, using $n_{H_2O} = 5I_{H_2O}/2(I_{3.1–4.1} - I_{H_2O})$. For glycerol, PG2 and PG3, n_{H_2O} = 0.12, 0.22 and 0.085, respectively. For the PG4 and PG6 samples, the water signal was too small and overlapped with other signals to be reliably estimated. As it was smaller than that of PG3, the water content of PG3 (n_{H_2O} = 0.085) was taken as an upper-bound estimate and applied to both samples. By normalizing $I_{C–H} = I_{3.1–4.1} - I_{H_2O}$ to a value of 5 (the number of carbon-bound protons per glycerol unit), the fractions of G, T, and L structures in each sample were calculated according to eqn (1)–(3):

$$L = I_L \quad (1)$$

 This journal is © The Royal Society of Chemistry 2026

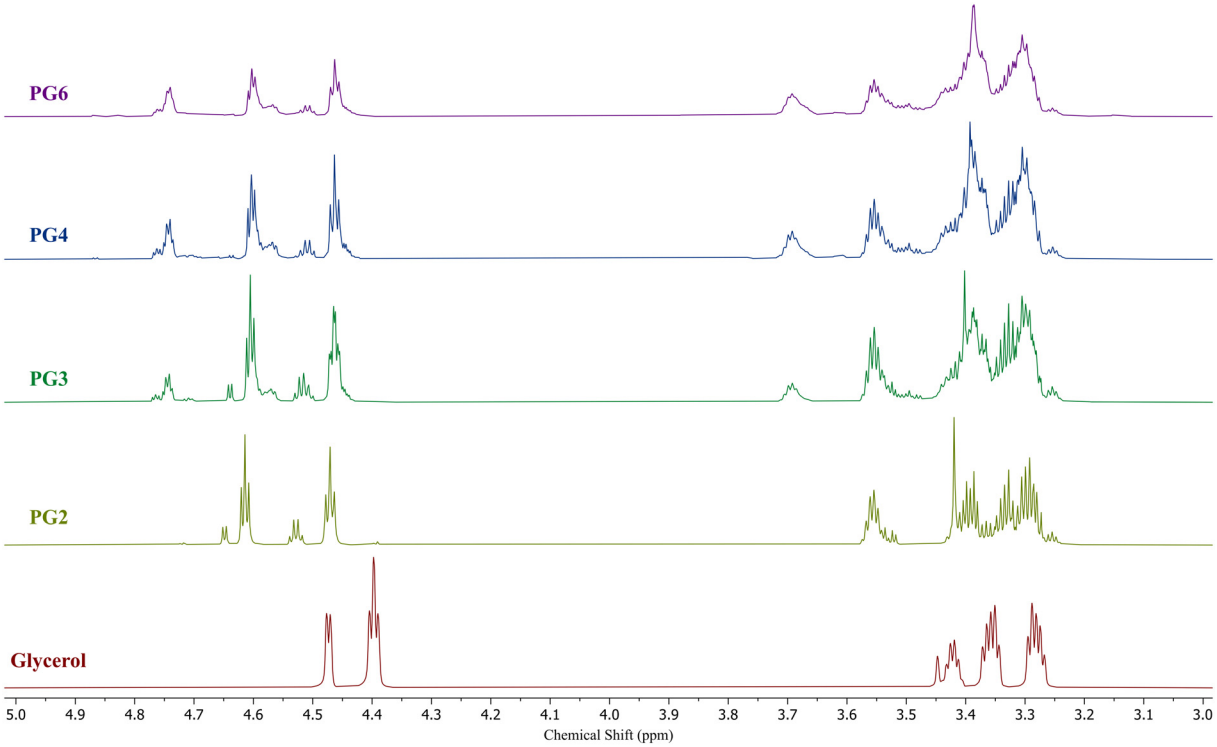


Fig. 6 Quantitative 800 MHz ^{1}H NMR spectra of glycerol and the four polyglycerol samples (PG2, PG3, PG4, and PG6) recorded in DMSO-d_6.

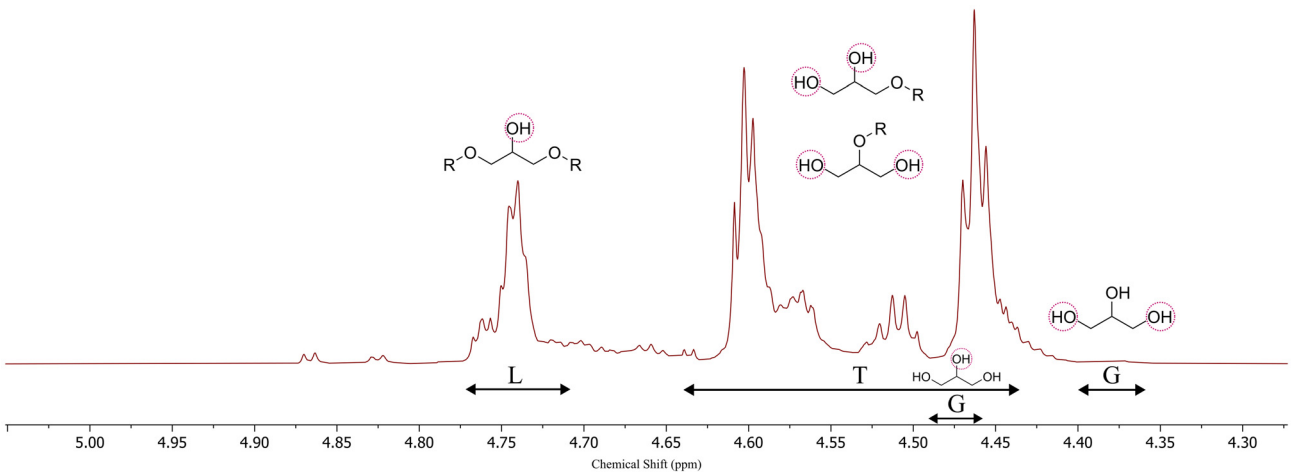


Fig. 7 Hydroxyl region of quantitative 800 MHz ^{1}H NMR spectra of the PG6 sample with marked regions according to the assignment of L, T and G, recorded in DMSO-d_6.

$$G = \frac{I_G}{2} \quad (2)$$

$$T = \frac{I_{T+G} - \frac{I_G}{2}}{2} \quad (3)$$

where I_L, I_G, and I_{T+G} are the normalized spectral integrals of the L, G, and T + G regions, respectively. Since each G unit contains two primary hydroxyl groups, the integral of the G region is divided by 2 to obtain its molar fraction. Similarly, since each terminal unit contains two hydroxyl groups, the remaining integral after subtracting the G contribution from the T + G region is divided by 2 to give the fraction of T structures. The results are presented in Table 4, where they are also compared to the composition determined by the ^{13}C NMR method, showing good agreement between the two approaches. It is important to note that as no Lsp or Lpp-ss substructures were identified in the analyzed samples, hence the chemical shift of

Table 4 Composition of the samples in terms of G, T and L structures, determined from ^{1}H (left) and ^{13}C NMR analysis (right)

	Quantity of each substructure based on integrals of OH in ^{1}H spectrum					Quantity of each substructure based on integrals of C signals in ^{13}C spectrum			
Sample	G	T	L	Unassigned (average OH per unit)	Sample	G	T	L	Unassigned
Glycerol	99%	1%	—	—	Glycerol	100%	—	—	—
PG2	2%	93%	3%	2% (0.9)	PG2	2%	96%	1%	1%
PG3	—	73%	20%	7% (0.5)	PG3	—	74%	18%	8%
PG4	—	58%	26%	16% (0.4)	PG4	—	58%	26%	15%
PG6	—	48%	27%	25% (0.4)	PG6	—	51%	27%	22%

their respective hydroxyl protons have not been established here. Therefore, some future additional assignments and subsequent modifications to the described strategy may be required for materials where these structures are present.

Some sources of error exist in the method, arising from factors such as baseline correction and water contribution, as illustrated by the pure glycerol sample where 1% of hydroxyl protons were determined as T, but overall, the presented protocol gives a robust composition determination in terms of glycerol, terminal and linear structures.

The unassigned hydroxyls, obtained by subtracting the assigned hydroxyl integrals from the total hydroxyl region, can be directly related to the unassigned glycerol units. This allows the average number of hydroxyls per unassigned unit to be estimated, see Table 4, providing insight into the nature of these units. This provides structural information about the unassigned fractions that is not accessible from ^{13}C NMR.

Although the ^{1}H NMR method does not provide the same level of structural detail as quantitative ^{13}C NMR, it offers a more straightforward approach, requiring only direct integration without the spectral deconvolution which is a necessity for the ^{13}C interpretation, and can provide a reliable indication of the relative fractions of linear and terminal units.

3 Conclusions

In this work, we have developed a comprehensive NMR-based methodology for detailed structural characterization of oligomeric polyglycerol (PG), enabling both assignment and quantification of glycerol substructures at an unprecedented level of detail. By combining multiple complementary NMR experiments (^{1}H, ^{13}C, DEPT-135, INADEQUATE, HSQC, and HMBC), we established a framework for resolving and assigning a large fraction of the carbon signalsin complex PG mixtures.

A key outcome of this study is the introduction of a substructure-based description of PG constitution, in which glycerol units are classified not only by their connectivity (G, T, L, D), but also by the nature of the linkages to neighboring units (primary *vs*. secondary carbons). This approach provides a significantly more nuanced representation of PG architecture compared to conventional assignment schemes, which often group broad spectral regions and thereby fail to capture the underlying structural diversity. Our comparison with literature data confirms that the present assignments are consistent with previous studies while offering enhanced structural resolution and interpretability, particularly for heterogeneous, low-molecular-weight samples.

Building on these assignments, we established a readily applicable quantitative ^{13}C NMR protocol for determining the relative abundance of individual substructures by systematic peak deconvolution. Application to four PG samples (PG2–PG6) revealed a clear compositional trend, with increasing chain length leading to a higher fraction of linear substructures. The predominance of Tp-p and Lpp-pp units confirms that the investigated materials are primarily composed of linearly connected glycerol units *via* primary carbons, in agreement with their synthesis from glycerol and the supplier specifications. At the same time, the increasing contribution of unresolved peaks with sample size highlights the rapidly expanding structural complexity of PG with increasing degree of polymerization.

Importantly, we also demonstrate that quantitative ^{1}H NMR can serve as a practical and accessible alternative for estimating overall composition, particularly the relative amounts of terminal and linear units. While this method does not provide the same level of structural detail as ^{13}C-based analysis, it offers a rapid and experimentally straightforward approach that yields results consistent with the more rigorous ^{13}C quantification.

Despite these advances, some limitations remain. Complete peak assignment was hindered by signal overlap and low-intensity signals. The observation that even identical substructures exhibit multiple chemical shifts underscores that PG constitution cannot be fully described by nearest-neighbor connectivity alone, but is influenced by a long-range structural context. Furthermore, dendritic and secondary-linked substructures (Lsp) could not be conclusively identified in the present samples, reflecting both their low abundance and the predominance of linear architectures in the studied materials.

Overall, this work provides a general and extensible framework for quantitative structural analysis of polyglycerol, bridging the gap between simplified compositional metrics and the true complexity of PG constitution. The methodology offers new opportunities to systematically investigate structure–property relationships in polyglycerol materials.

Future work should aim to extend this approach to highly branched and dendritic PG, where the full diversity of substructures can be explored, as well as to correlate the detailed constitutional information obtained here with macroscopic

 This journal is © The Royal Society of Chemistry 2026

properties of PG-based materials such as surfactants or in biomedical applications.

4 Materials and methods

4.1 Materials and sample preparation

Four different oligomeric polyglycerol products of different size distributions were provided by Spiga Nord S.p.A (Carasco, Italy): pure vegetable polyglycerine-6 (PG6), pure vegetable polyglycerine-4 (PG4), pure vegetable polyglycerine-3 (PG3) and pure vegetable diglycerine (PG2). The polyglycerol materials are described by the supplier as having a high proportion of linear structures with minimal cyclic content, and were all synthesized by condensation of glycerol.[39] The PG2 sample is described as mainly diglycerol, the PG3 sample is mainly 2, 3, and 4 glycerol units per molecule, the PG4 sample as mainly 3, 4 or 5 glycerol units per molecule and the PG6 sample as mainly 3, 4, 5, 6 units and longer chains. More details about the sample size distributions given by the supplier can be found in the SI.

Glycerol (≥99.0%, Sigma) and fully deuterated dimethyl sulfoxide (DMSO-d_6) (99.9 atom% D, Acros Organics) were used without further purification.

NMR samples were prepared in DMSO-d_6 with 60 mg sample in 600 μL solvent for ^{1}H, ^{13}C and DEPT-135, and 180 mg sample in 600 μL solvent for INADEQUATE, HSQC and HMBC.

4.2 NMR spectroscopy

All NMR experiments were performed at room temperature on an 800 MHz Bruker Avance III HD spectrometer (Oxford magnet) equipped with a 5 mm TXO cryoprobe and a SampleJet sample changer. The DMSO solvent signal was used as the reference to calibrate the spectra (39.52 ppm for ^{13}C and residual ^{1}H at 2.50 ppm), and the ^{1}H and ^{13}C 90° pulse lengths were calibrated to 10.2 μs and 12.7 μs, respectively. A combination of one- and two-dimensional experiments was employed, comprising ^{1}H, ^{13}C, DEPT-135, HSQC, HMBC, and INADEQUATE. DEPT-135 was used to distinguish between CH and CH_2 groups, whereas HSQC and HMBC established one-bond and long-range ^{1}H–^{13}C correlations, respectively. Direct ^{13}C–^{13}C connectivities were traced using INADEQUATE, allowing unambiguous carbon–carbon assignment. Acquisition parameters for each experiment, including the number of scans (NS), time domain points (TD), relaxation delay (D_1), spectral width (SW), and coupling constant (J), are provided in the SI.

To determine the fraction of each glycerol substructure in the polyglycerol, quantitative ^{1}H 1D spectra and ^{13}C inverse-gated 1D spectra were acquired. Since quantitative NMR requires complete relaxation of all signals between successive scans, accurate T_1 values must be known. T_1 relaxation times were measured on glycerol rather than on polyglycerol. This choice was made because glycerol represents the smallest and most mobile glycerol-based species expected in the samples and is therefore expected to exhibit the longest T_1 relaxation times. Using a relaxation delay of $D_1 = 5 \times T_1$(glycerol) thus provides a conservative criterion that ensures complete relaxation of the polyglycerol resonances and the validity of quantitative measurements. Note that inverse-gated ^{1}H decoupling was employed during acquisition to suppress NOE effects, ensuring that the ^{13}C signal integrals are proportional to the number of contributing nuclei.

4.3 NMR peak assignment and constitution analysis

A systematic multi-experiment approach was employed for reliable signal assignments. The methodology is the following:

- The DEPT-135 ^{13}C NMR spectra enabled to distinguish CH and CH_2 carbons based on their phase response, giving an initial picture of the carbon multiplicities in the polyglycerol backbone and substituent chains. By comparing with the chemical shifts from ref. 38 we could identify the CH-OH, CH-OR, CH_2-OH, and CH_2-OR groups.
- The INADEQUATE ^{13}C^{13}C spectra allowed to determine ^{13}C–^{13}C correlations. However, not all correlations could be picked up in this experiment, mainly due to its inherent low sensitivity, which stems from the low natural abundance of ^{13}C.
- HSQC and HMBC ^{1}H^{13}C experiments were used to identify the low intensity signals (*i.e.*, not identified with the INADEQUATE experiment). HSQC was used to identify one-bond carbon-proton correlations ($^1J_{CH}$), while HMBC provided long-range carbon-proton correlations ($^nJ_{CH}$).
- HSQC was further used to assign the ^{1}H NMR peaks, by identifying the protons directly attached to each carbon based on the established ^{13}C assignments.

For ^{13}C NMR, integrals were determined by peak deconvolution with a Lorentzian signal shape for the fitting, for peaks with a signal-to-noise ratio greater than 3.5. The sum of the integrals of all deconvoluted peaks was normalized to 1 for the ^{13}C spectra. For the ^{1}H spectra, integrals were taken over specific regions without deconvolution.

Conflicts of interest

There are no conflicts to declare.

Data availability

The data supporting this article have been included as part of the supplementary information (SI). Supplementary information is available. See DOI: https://doi.org/10.1039/d6py00638h.

Acknowledgements

Spiga Nord S.p.A are acknowledged for kindly providing the polyglycerol samples. The NMR measurements were carried out at the Swedish NMR Centre, Göteborg, Sweden.

References

1 C. A. Pagnacco, A. Alvarez-Fernandez, A. Maestro, E. G. de San Román, R. Lund and F. Barroso-Bujans, *Macromol. Rapid Commun.*, 2025, **46**, 2400791.
2 R. K. Kainthan, E. B. Muliawan, S. G. Hatzikiriakos and D. E. Brooks, *Macromolecules*, 2006, **39**, 7708–7717.
3 R. K. Kainthan, J. Janzen, E. Levin, D. V. Devine and D. E. Brooks, *Biomacromolecules*, 2006, **7**, 703–709.
4 P. Pouyan, M. Cherri and R. Haag, *Polymers*, 2022, **14**, 2684.
5 A. Thomas, S. S. Müller and H. Frey, *Biomacromolecules*, 2014, **15**, 1935–1954.
6 M. Calderón, M. A. Quadir, S. K. Sharma and R. Haag, *Adv. Mater.*, 2010, **22**, 190–218.
7 H. Frey and R. Haag, *Rev. Mol. Biotechnol.*, 2002, **90**, 257–267.
8 Y. Shen, X. He and L. Chen, *Biosensors*, 2025, **15**, 502.
9 Y. Qi and A. Chilkoti, *Curr. Opin. Chem. Biol.*, 2015, **28**, 181–193.
10 R. Ciriminna, B. Katryniok, S. Paul, F. Dumeignil and M. Pagliaro, *Org. Process Res. Dev.*, 2015, **19**, 748–754.
11 J. P. M. Andal, R. R. Navarro and R. D. Maalihan, *Macromol*, 2025, **5**, 48.
12 M. Tryznowski, Z. Żołek-Tryznowska and J. Izdebska-Podsiadły, *J. Coat. Technol. Res.*, 2018, **15**, 649–655.
13 M. Zhang and G. Zhang, *Polymers*, 2025, **17**, 879.
14 S. Damle and C. Madankar, *Tenside, Surfactants, Deterg.*, 2023, **60**, 611–621.
15 V. Norn, in *Polyglycerol Esters*, 2014, pp. 181–208.
16 D. H. A. de Brito, A. P. D. Schuller, I. M. Cavalcante, N. R. C. Rocha, D. R. Moreira, M. E. Maier, C. L. Petzhold and N. M. P. S. Ricardo, *J. Am. Oil Chem. Soc.*, 2025, **102**, 71–82.
17 GVR Personal Care & Cosmetics Research Team, *Polyglycerol Market Size and Share Industry report, 2033*, https://www.grandviewresearch.com/industry-analysis/polyglycerol-market, 2025, [online; accessed 03-June-2026].
18 E. Mohammadifar, A. N. Kharat and M. Adeli, *J. Mater. Chem. B*, 2015, **3**, 3896–3921.
19 S. Salehpour and M. A. Dubé, *Macromol. Chem. Phys.*, 2011, **212**, 1284–1293.
20 International Agency for Research on Cancer, in *IARC Monographs on the Evaluation of Carcinogenic Risks to Humans - Some Industrial Chemicals*, IARC, Lyon, France, 2000, vol. 77 of IARC Monographs on the Evaluation of Carcinogenic Risks to Humans.
21 G. Rokicki, P. Rakoczy, P. Parzuchowski and M. Sobiecki, *Green Chem.*, 2005, **7**, 529–539.
22 M. Bochenek, N. Oleszko-Torbus, W. Wałach, D. Lipowska-Kur, A. Dworak and A. Utrata-Wesołek, *Polym. Rev.*, 2020, **60**, 717–767.
23 C. Schubert, M. Schömer, M. Steube, S. Decker, C. Friedrich and H. Frey, *Macromol. Chem. Phys.*, 2018, **219**, 1700376.
24 A. Bhargava, S. Shelke, M. Dilkash, N. S. Chaubal-Durve, P. D. Patil, S. S. Nadar, D. Marghade and M. S. Tiwari, *Rev. Chem. Eng.*, 2023, **39**, 1187–1226.
25 M. Ionescu and Z. S. Petrović, *Eur. J. Lipid Sci. Technol.*, 2018, **120**, 1800004.
26 C. C. Chong, A. Aqsha, M. Ayoub, M. Sajid, A. Z. Abdullah, S. Yusup and B. Abdullah, *Environ. Technol. Innovation*, 2020, **19**, 100859.
27 T. N. Kumar, Y. S. R. Sastry and G. Lakshminarayana, *J. Am. Oil Chem. Soc.*, 1989, **66**, 153–157.
28 A. Martin and M. Richter, *Eur. J. Lipid Sci. Technol.*, 2011, **113**, 100–117.
29 M. Imran ul-haq, B. F. L. Lai, R. Chapanian and J. N. Kizhakkedathu, *Biomaterials*, 2012, **33**, 9135–9147.
30 S.-E. Stiriba, H. Kautz and H. Frey, *J. Am. Chem. Soc.*, 2002, **124**, 9698–9699.
31 M. Yamazaki, Y. Sugimoto, D. Murakami, M. Tanaka and T. Ooya, *Langmuir*, 2021, **37**, 8534–8543.
32 E. Vandenberg, in *Coordination polymerization*, Springer, 1983, pp. 11–43.
33 E. J. Vandenberg, *J. Polym. Sci., Polym. Chem. Ed.*, 1985, **23**, 915–949.
34 R. Tokar, P. Kubisa, S. Penczek and A. Dworak, *Macromolecules*, 1994, **27**, 320–322.
35 A. Dworak, W. Walach and B. Trzebicka, *Macromol. Chem. Phys.*, 1995, **196**, 1963–1970.
36 A. Sunder, R. Hanselmann, H. Frey and R. Mülhaupt, *Macromolecules*, 1999, **32**, 4240–4246.
37 B. R. Spears, M. A. Marin, J. R. Montenegro-Burke, B. C. Evans, J. McLean and E. Harth, *Macromolecules*, 2016, **49**, 2022–2027.
38 S. Cassel, C. Debaig, T. Benvegnu, P. Chaimbault, M. Lafosse, D. Plusquellec and P. Rollin, *Eur. J. Org. Chem.*, 2001, 875–896.
39 Spiga Nord S.p.A, *About polyglycerols*, https://www.spiga-nord.com/spiga-nord-polyglycerols-pure-vegetable-kosher-grade-polyglycerine/#polyglycerols, c 2006–2024, [online; accessed 16-June-2026].

This journal is © The Royal Society of Chemistry 2026